Available online at www.sciencedirect.com
SCIENCE DIRECT®
ELSEVIER
Journal of Magnetism and Magnetic Materials 277 (2004) 130–135
Journal of magnetism and magnetic materials
www.elsevier.com/locate/jmmm

Is Heusler compound Co_2CrAl a half-metallic ferromagnet: electronic band structure, and transport properties

Ming Zhang[a,*], Zhuhong Liu[a], Haining Hu[a], Guodong Liu[a], Yuting Cui[a], Jinglan Chen[a], Guangheng Wu[a], Xixiang Zhang[b], Gang Xiao[c]

[a] *State Key Laboratory for Magnetism, Institute of Physics, Chinese Academy of Sciences, P.O. Box 603, Beijing 100080, People's Republic of China*

[b] *Department of Physics, The Hong Kong University of Science and Technology, Clear Water Bay, Kowloon, Hong Kong, People's Republic of China*

[c] *Physics Department, Brown University, Providence, RI 02912, USA*

Received 2 September 2003; received in revised form 21 October 2003

Abstract

We report the electronic band structure, and transport properties of the Heusler compound Co_2CrAl. The band structure calculation shows that Co_2CrAl is a true half-metallic ferromagnet with a magnetic moment of $3\,\mu_B$ per formula, characterized by a full indirect band gap of 0.475 eV at around the Fermi level in the minority-spin band. The electronic resistivity shows a power-law $T^{3.15}$ temperature dependence at low temperatures ascribed to the unconventional one-magnon scattering processes. A negative MR maximum of –0.33% is obtained for Co_2CrAl at 300 K.

PACS: 71.20.Lp; 72.15.Eb; 75.47.Np

Keywords: Band structure; Transport property; Heusler alloy

1. Introduction

The rapidly developing field of spintronics [1,2] holds much promise for the future. Widely possible applications are in non-volatile magnetic random access memories, but also an increase of the efficiency of the optoelectronic devices and even a self-assembled quantum computer are envisaged [3]. In particular, most magnetoelectronic devices rely on an imbalance in the number of majority- and minority-spin carriers, with the ideal material exhibiting a complete (100%) spin polarization at the Fermi level (i.e., a half-metallic ferromagnet—HMF) [4]. Within this framework, the first HMF was predicted by de Groot et al. [4], in the Heusler alloys in 1983; in succession, some Heusler alloys have been theoretical predicted as HMFs with a unity spin polarization [4–8]. Much effort has been paid to investigate the mechanism behind the HM magnetism and to study its

*Corresponding author. Tel.: +861082649247; fax: +861082649485.
E-mail address: zm_info@yahoo.com.cn (M. Zhang).

0304-8853/$ - see front matter © 2003 Elsevier B.V. All rights reserved.
doi:10.1016/j.jmmm.2003.10.017

implication in various physical properties. At the same time, great effort is being made to find new members of this family of HMFs, which are more promising for applications. This has motivated us to investigate the electronic band structure, and transport properties of the Heusler compound Co_2CrAl. Although the magnetic properties were reported by Buschow et al. [9], the transport measurement and the electronic band structure calculation can give us a deeper understanding of this compound.

2. Computational and experimental details

The full-potential linearized augmented plane wave plus local orbitals method based on the local spin density approximation for the exchange-correlation potential within the framework of DFT [10] was used in our calculations, where the potential and charge density are treated with no shape approximation. The relativistic effect was taken into consideration in the scalar style, but the spin–orbital coupling was neglected. The muffin-tin sphere radii R used were both 2.4 a.u. for Co, Cr and Al atoms. Inside the atomic spheres the charge density and the potential were expanded in crystal harmonics up to $l = 6$. The radial basis functions of each linearized augmented plane wave were calculated up to $l = 8$ and the non-spherical potential contribution to the Hamilton matrix had an upper limit of $l = 4$. The Brillouin-zone integration was done with a modified tetrahedron method [11] and we used 3000 k-points in the irreducible part of the Brillouin zone (IBZ). The density plane-wave cutoff was $RK_{\max} = 8.0$. The self-consistency was better than 0.001 me/a.u.^{3} for charge density and spin density, and the stability was better than 0.01 mRy for the total energy per cell.

The ordered alloy Co_2CrAl was prepared by repeated melting of appropriately composed mixture of high-purity metals (Co, Cr and Al with 3N or better) in an arc furnace under argon atmosphere. The weight loss during melting was small. Subsequently, the ingots were annealed in vacuum at 800°C for 5 days and cooled down to room temperature. The resistivity and the magnetoresistance (MR) measurements were carried out using the four-point DC technique in a commercial superconducting quantum interference device magnetometer.

3. Results and discussion

3.1. Electronic structure

In Fig. 1, we have gathered the spin-dependent total and partial DOS for Co_2CrAl. As seen in Fig. 1, the valence band extends more than 5 eV below the Fermi level. In the majority-spin component, Cr *3*d states are occupied and hybridized with Co *3*d electrons; on the other hand, in the minority-spin part, local and mostly

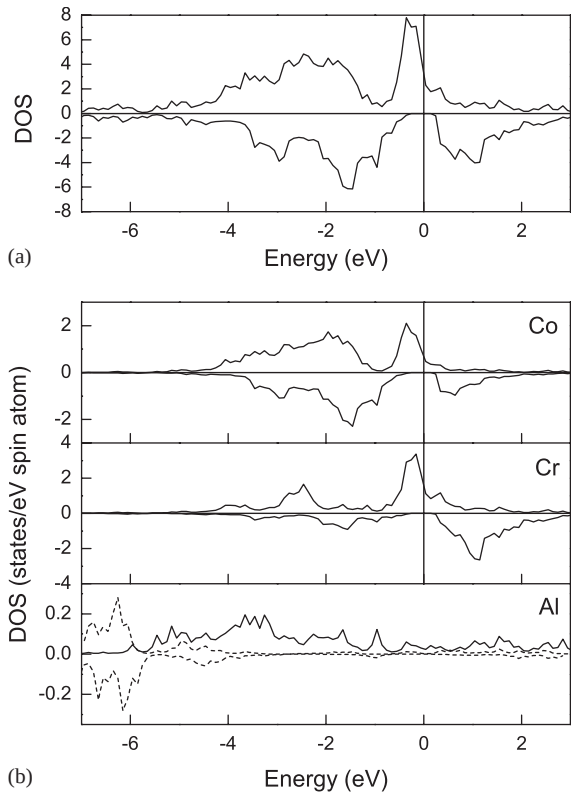

Fig. 1. The spin-dependent total DOS (a), and partial DOS (b) plots for Co_2CrAl. (a) (—) total DOS; (b) partial DOS plots, (- - -) s orbitals, (—) the p orbitals of Al atoms or the d orbitals of Co and Cr atoms. The Fermi level is defined as the zero point of the energy axis.

non-hybridized Cr *3*d states are found at about 1.1 eV above E_F. The Al atom provides s–p states to be hybridized with d electrons and determines the degree of occupation of p–d orbitals. It is clear that the majority-spin electrons are metallic whereas there is an energy gap of about 0.475 eV around the Fermi level in the bands for the minority-spin electrons. Thus, Co_2CrAl is a typical HMF. The magnetic moments of the atoms Co, Cr, and Al are 0.650 μ_B, 1.745 μ_B, and –0.045 μ_B, respectively. Thus the total spin magnetic moment is 3.000 μ_B per formula unit, which is equal to an integral number of Bohr magneton expected for an HMF. From the density of states at the Fermi level ($N(E_F) = 3.292$ states/eV·cell) of the both spin bands and using independent-electron theory, the coefficient γ of the electronic specific heat ($C = \gamma T$) has been estimated as $\gamma = 7.76\,\mathrm{mJ/mol\,deg^2}$.

Furthermore, we present the spin-dependent energy bands along high-symmetry directions in the Brillouin zone, as shown in Fig. 2. The main characters of our results are similar with several other calculations of electronic structure of the half-metallic full-Heusler alloys [12,13]. Furthermore, the discussion on the electronic band structure of the full-Heusler alloys can be found analytically in Ref. [12]. With the help of the DOS, it is clear that the energy region that is lower than –3 eV consists mainly of s and p electrons of the Al atoms and the band structure is almost identical for both spin directions, and the energy region between –3 and 2 eV consists mainly of the d electrons of Co and Cr atoms. In particular, the Al s electrons transform following the Γ_1 representation at the Γ point, being unaffected by the Co and Cr exchange interaction; we do not show this band in Fig. 2 as it very low in energy and it is well separated by the other bands. The upper dispersed bands are due to the strong hybridization of Cr d and Co d electrons, including a contribution from Al p states in the occupied valence states. The p electrons of the Al atom transform following the Γ_{15} representation and they hybridize with p electrons of the Cr and Co atoms, which transform with the same representation. Above this point there is a double-degenerated Γ_{12} point which corresponds to the e_g orbitals. The Co e_g orbitals with Γ_{12}' symmetry above the Fermi level cannot

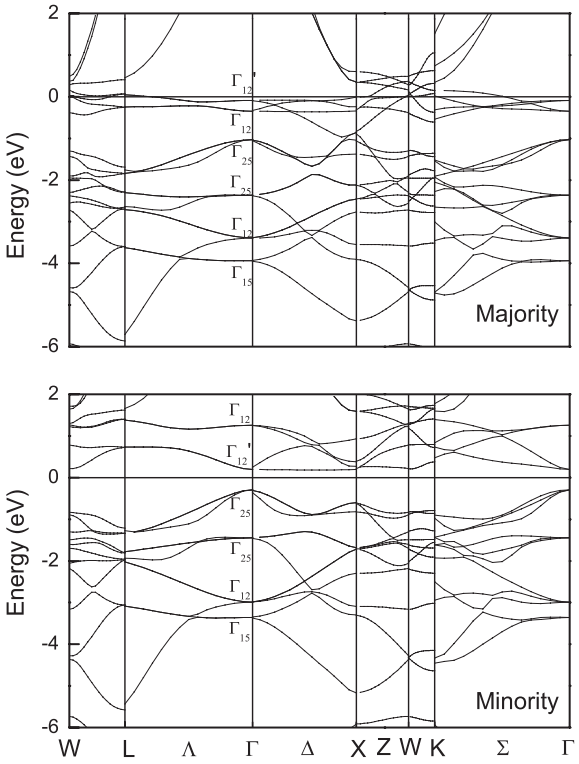

Fig. 2. The band structure of Co_2CrAl at the experimental lattice constant of 0.573 nm.

mix with others, as leads to the Γ_{12}' bands rather flat. In the cubic crystal field, the Cr d states are spit into a doublet with e_g (Γ_{12}) symmetry and a triplet with t_{2g} (Γ_{25}) symmetry, respectively. They will hybridize with Co d orbitals with the same symmetry. From the observation, these Γ_{25} and Γ_{12} levels are below and above the Fermi energy, respectively.

The majority-spin band structure is strongly metallic, while the minority-spin band structure shows a semiconducting gap around the Fermi level. The calculated indirect Γ–X band gap for minority carriers is 0.475 eV, while the Fermi level lies 0.294 eV above the highest minority-spin valence bands. Hence, the "spin-flip gap (HM gap)", i.e., the minimum energy required to flip a minority-spin electron from the valence band maximum to the majority-spin Fermi level, is of 0.181 eV. The non-zero HM gap implies that Co_2CrAl is a true HMF. The band gap in the

minority bands basically arises from the covalent hybridization between the d states of the Co and Cr atoms, leading to the formation of bonding and antibonding bands with a gap in between, as is illustrated in detail in Refs. [12–14]. It is worth noting that in our calculations the spin–orbital coupling is not taken into account, which can slightly lift the band degeneracy. However, when the calculated indirect gap is sufficiently large, the spin–orbit coupling does not destroy the half-metallicity.

3.2. Structure

Fig. 3 shows the X-ray diffraction pattern (XRD) of the sample, which is consistent with what is expected from a single-phase sample. All diffraction lines can be indexed with the cubic structure. Ordering of the Cr and Al sublattice is indicated by the presence of the (1 1 1) superlattice diffraction peak and ordering of the Co sublattice is indicated by the presence of the (2 0 0) superlattice peak. The presence of both (1 1 1) and (2 0 0) peaks confirms the $L2_1$ structure. The lattice parameter was found to be $a = 5.74 \pm 0.03$ Å, consistent with earlier work [9]. In general, the degree of atomic disordering can be estimated by comparing the experimental values of relative intensities of even ($h + k + l = 4n + 2$) and odd (h, k, l = all odd) superstructure lines of $L2_1$ structure with those expected from ideal atomic ordering. But, in practice, measuring disorder between Co and Cr sublattices with XRD is extremely difficult due to the little difference of the scattering factor between Co and Cr atoms.

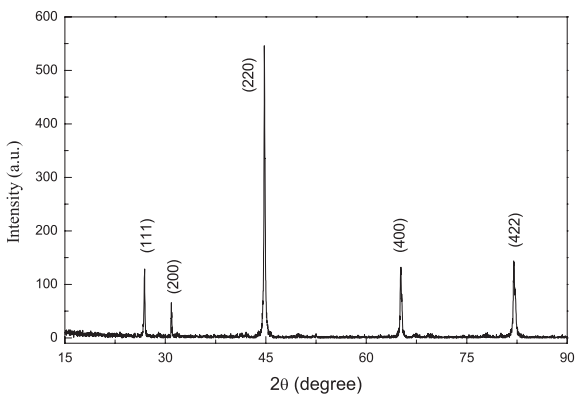

Fig. 3. XRD spectra for Co_2CrAl.

3.3. Transport properties

The resistivity ρ as a function of temperature is shown in Fig. 4(a). The resistivity decreases upon the temperature decreasing and characters a typical metallic behavior. The striking character of the data is that the residual resistivity is quite large (56 μΩ cm), while the overall variation with temperature is weak. The compound has a residual resistivity ratio (RRR) of 1.1, whose magnitude is much lower than that of Co_2MnSi single crystal, 6.5 [15]. Small amount of defects and impurities can have dramatic effects on the RRR, and as for the Heusler compounds, a reduced RRR can result from scattering contributions from impurities or

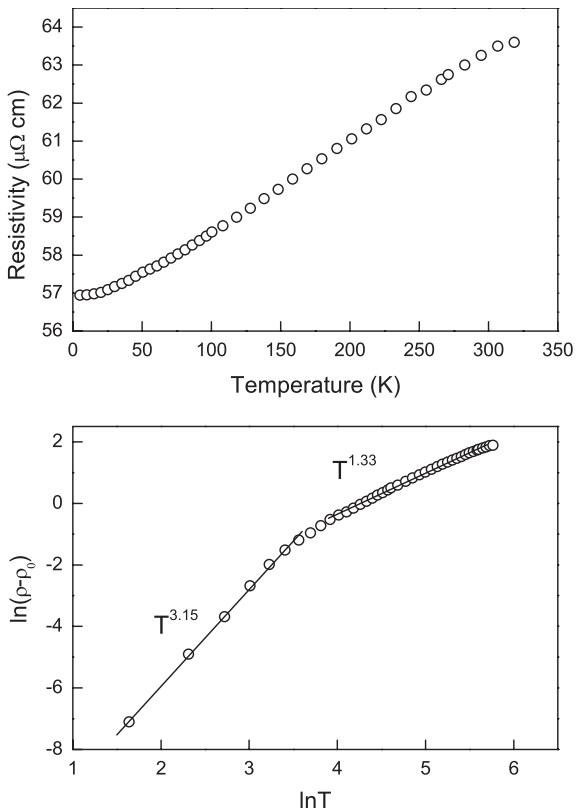

Fig. 4. (a) ρ vs. T plot for Co_2CrAl, and (b) $\ln(\rho - \rho_0)$ vs. $\ln(T)$ plot.

antisite defects. Raphael et al. [15] reported a Co–Mn antisite disorder of around 10–14% for the arc-melted sample of Co_2MnSi whose RRR has a magnitude of 2.7. Therefore, it is a reasonable estimation that there exist a relatively large amount of antisite defects in Co_2CrAl. Since Orgassa et al. [16] reported that for NiMnSb only 5% disorder can move the Fermi level outside of the gap or lead to the gap disappearance, here the disorder defects in Co_2CrAl can possibly have a remarkable effect on the half-metallicity and the electronic transport properties.

An analysis of the resistivity data for Co_2CrAl is given in Fig. 4(b). By assuming the functional form $\rho = \rho_0 + cT^n$ for our data, a plot of $\ln(\rho-\rho_0)$ as a function of $\ln(T)$ will yield a curve whose slope corresponds to the exponent n. Our analysis shows that the resistivity ρ behaves according to $a \sim T^{3.15}$ power law in the critical low-temperature region $T < 35\,\mathrm{K}$, and afterwards the dependence transforms from a $T^{3.15}$ dependence to a $T^{1.33}$ behavior upon temperature increase.

In the conventional metallic ferromagnets the contribution of the magnetic scattering to the low-temperature transport properties is governed primarily by the one-magnon scattering processes, which give rise to a T^2 temperature dependence due to absorption and emission of a single magnon [17]. For HMFs, conduction electrons are perfectly spin-polarized, and the Fermi surface is absent in the minority bands. Based on the rigid-band picture, Kubo and Ohata [18] have shown that while one-magnon processes are exponentially suppressed by a factor $\exp(-E_g/k_BT)$, where E_g is the minority-spin band gap at the Fermi level, the two-magnon processes can lead to a $T^{9/2}$ temperature dependence. However, Furukawa [17] have shown that resistivity is strongly influenced by spin fluctuations. At a finite temperature, spin fluctuations induce a minority band and once the thermally activated minority band is created and occupied, the unconventional one-magnon scattering processes are allowed, which can lead to a T^3 temperature dependence [17]. It is clear that the resistivity of Co_2CrAl at low temperature agrees well with the theory of the unconventional one-magnon scattering processes. At higher temperatures, there does not exist any new character for the resistivity behavior of Co_2CrAl with respect to the ordinary ferromagnets.

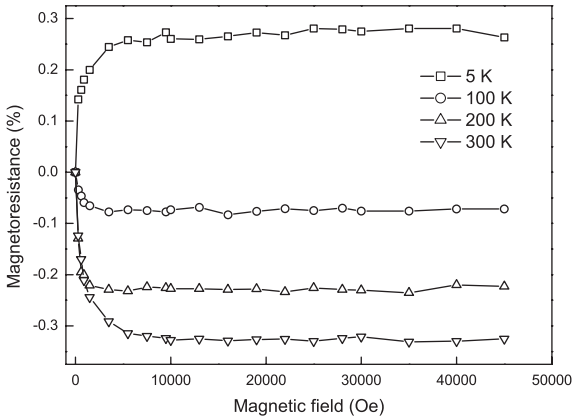

Fig. 5. MR as a function of the magnetic field at 5, 100, 200, and 300 K.

In magnetic alloys, the MR reflects the reduction in magnetic disorder caused by the application of a magnetic field at a given temperature [19]. Fig. 5 shows that at low-temperatures MR is positive, but is increasingly dominated by a negative component as temperature increases, and the MR of Co_2CrAl at 300 K is -0.33%. The behavior in Fig. 5 can be interpreted in terms of the competition between the positive contribution, due to the effect of the Lorentz force during the itinerant electrons mean free path, and a negative contribution due to the extinction of inelastic s–d–s scattering as the magnetic field increases [20,21]. At the lowest temperature, the inelastic scattering is at a minimum and MR is dominated by the positive contribution; increasing the temperature reduces the positive contribution to MR and increases the negative component of MR because the new inelastic scattering channels are opened [21].

4. Summary

We have studied the electronic band structure, and the transport properties of Co_2CrAl. Co_2CrAl is predicted to be a true HMF with a magnetic moment of $3.0\,\mu_B$ per formula unit and a spin-flip gap of 0.181 eV by the electronic band structure calculations. Temperature dependence of resistivity

for Co_2CrAl reveals a small RRR ($\rho_{300\,K}/\rho_{5\,K}$), which reflects the relatively large amount of Co–Cr antisite defects. The electronic resistivity shows a $T^{3.15}$ power-law temperature dependence, which may be attributed to the unconventional one-magnon process by considering the spin-fluctuations beyond the rigid-band approximation outlined by Furukawa [17] A negative MR maximum of –0.33% is obtained for Co_2CrAl at 300 K.

Acknowledgements

This work is supported by National Natural Science Foundation of China Grant No. 50201020 and 50271083. X.X. Zhang and G.H. Wu would like to thank the financial support from the Research Grants Council of the Hong Kong Special Administration Region, China (Project No. HKUST6059/02E).

References

[1] G.A. Prinz, Phys. Today 48 (1995) 58.
[2] K.I. Kobayashi, T. Kimura, H. Sawada, K. Terakura, K. Tokura, Nature (London) 395 (1998) 677.
[3] S. Bandyopadhyay, Phys. Rev. B 61 (2000) 13813.
[4] R.A. de Groot, F.M. Mueller, P.G. van Engen, K.H.J. Buschow, Phys. Rev. Lett. 50 (1983) 2024.
[5] R.A. de Groot, K.H.J. Buschow, J. Magn. Magn. Mater. 13 (1986) 1377.
[6] S. Fujii, S. Inshida, S. Asano, J. Phys. Soc. Japan 64 (1995) 185.
[7] M.J. Otto, R.A.M. van Woerden, P.J. van Valk, J. Wijngaard, C.F. van Bruggen, C. Haas, J. Phys.: Condens. Matter 1 (1989) 2351.
[8] C. Jiang, M. Venkatesan, J.M.D. Coey, Solid State Commun. 118 (2001) 513.
[9] K.H.J. Buschow, P.J. van Engen, J. Magn. Magn. Mater. 25 (1981) 90.
[10] U. von Barth, L. Hedin, J. Phys. C 5 (1972) 1692; P. Hohenberg, W. Kohn, Phys. Rev. 136 (1964) B864; P. Blaha, K. Schwarz, P. Sorantin, S.B. Tricky, Comput. Phys. Commun. 59 (1990) 399.
[11] P. Blöchl, O. Jepson, O.K. Andersen, Phys. Rev. B 49 (1994) 16223; S. Blugel, H. Akai, R. Zeller, P.H. Dederichs, Phys. Rev. B 35 (1987) 3271.
[12] I. Galanakis, P.H. Dederichs, N. Papanikolaou, Phys. Rev. B 66 (2002) 174429.
[13] S. Picozzi, A. Continenza, A.J. Freeman, Phys. Rev. B 66 (2002) 094421.
[14] I. Galanakis, P.H. Dederichs, N. Papanikolaou, Phys. Rev. B 66 (2002) 134428.
[15] M.P. Raphael, B. Huang, M.A. Willard, S.F. Cheng, B.N. Das, R.M. Stroud, K.M. Bussmann, J.H. Claassen, V.G. Harris, Phys. Rev. B 66 (2002) 104429.
[16] D. Orgassa, H. Fujiwara, T.C. Schulthess, W.H. Butler, Phys. Rev. B 60 (1999) 13237.
[17] N. Furukawa, J. Phys. Soc. Japan 69 (2000) 1954.
[18] K. Kubo, N. Ohata, J. Phys. Soc. Japan 33 (1972) 21.
[19] A. Hamzic, R. Asomoza, I.A. Campbell, J. Phys. F 11 (1981) 1441.
[20] M.T. Beal-Monod, R.A. Weiner, Phys. Rev. 170 (1968) 552.
[21] S.P. McAlister, I. Shiozaki, C.M. Hurd, C.V. Stager, J. Phys. F 11 (1981) 2129.